molecular pharmaceutics

articles

Insulin-Loaded Microcapsules for In Vivo Delivery

Byung Soo Kim,[†,‡] Jae Min Oh,[†,‡] Hoon Hyun,[†,‡] Kyung Sook Kim,[‡] Sang Hyo Lee,[‡,§] Yu Han Kim,[‡] Kinam Park,[||] Hai Bang Lee,[*,‡] and Moon Suk Kim[*,‡,§]

Fusion Biotechnology Research Center, Korea Research Institute of Chemical Technology, P.O. Box 107, Yuseong, Daejeon 305-600, Korea, and Departments of Biomedical Engineering and Pharmaceutics, Purdue University, 206 S. Intramural Drive, West Lafayette, Indiana 47907-1791

Received July 9, 2008; Revised Manuscript Received December 4, 2008; Accepted December 10, 2008

Abstract: Microencapsulation of insulin has been difficult, due to the high sensitivity of insulin to the harsh conditions that can occur during the microencapsulation process. We have developed a method of preparing insulin-loaded microcapsules by using a monoaxial ultrasonic atomizer to form microdroplets of insulin in aqueous solution surrounded by poly(lactic-*co*-glycolic acid) (PLGA) solution. Administration of these insulin-loaded microcapsules to type 1 diabetic rats maintained plasma insulin concentrations for 30 days, due to the sustained insulin release properties of the microcapsules. In contrast, plasma insulin concentrations after subcutaneous injection of insulin solution reached near zero levels within 2 days. Insulin solution showed only an immediate pharmacological effect, with no reduction of glycemia after 3 days, whereas insulin-loaded microcapsules maintained blood glucose levels at 100−200 mg/dL for 55 days. Molecular imaging using fluorescein isothiocyanate (FITC)-insulin-loaded microcapsules showed in vivo sustained release of the FITC-insulin in microcapsules. Using insulin-loaded microcapsules, we observed inflammation only immediately after injection, indicating that the rats adapted to long-term insulin release. In conclusion, insulin-loaded microcapsules may reduce nonrepetitive insulin administration and show sustained pharmacological performance.

Keywords: Insulin; microcapsule; transplantation; molecular imaging; inflammation

1. Introduction

Insulin therapy is important in the treatment of patients with insulin-dependent diabetes mellitus (type 1) and for many patients with noninsulin-dependent diabetes mellitus (type 2).[1,2] Patients with type 1 diabetes must self-administer insulin subcutaneously single or multiple times per day. Insulin treatment is also required during the later stages of type 2 diabetes to maintain glycemic control. Frequent injection, along with the pain, tenderness, local tissue necrosis, microbial contamination, and nerve damage associated with frequent subcutaneous insulin injections, have prompted research on alternative therapies.[3,4]

* Corresponding author. E-mail: mskim@krict.re.kr (M.S.K.); hblee@krict.re.kr (H.B.L.). Telephone: 82-42-860-7095. Fax: 82-42-860-7228. Current address for M.S.K.: Department of Molecular Science and Technology, Ajou University, Suwon 443-759, Korea; e-mail, moonskim@ajou.ac.kr.

† These authors are equal first authors in this work.

‡ Korea Research Institute of Chemical Technology.

§ Current address: Department of Molecular Science and Technology, Ajou University, Suwon 443-759, Korea.

|| Purdue University.

(1) Puigserver, P.; Rhee, J.; Donovan, J.; Walkey, C. J.; Yoon, J. C.; Oriente, F.; Kitamura, Y.; Altomonte, J.; Dong, H.; Accili, D.; Spiegelman, B. M. Insulin-regulated hepatic gluconeogenesis through FOXO1-PGC-1α interaction. *Nature* **2003**, *423*, 550–555.

(2) Evans, M. Avoiding hypoglycaemia when treating type 1 diabetes. *Diabetes, Obes. Metab.* **2005**, *7*, 488–492.

(3) Hinchcliffe, M.; Illum, L. Intranasal insulin delivery and therapy. *Adv. Drug Delivery Rev.* **1999**, *35*, 199–234.

(4) Muchmore, D. B.; Gates, J. R. Inhaled insulin delivery--where are we now. *Diabetes, Obes. Metab.* **2006**, *8*, 634–642.

(5) Jeong, B.; Kim, S. W.; Bae, Y. H. Thermosensitive sol-gel reversible hydrogels. *Adv. Drug Delivery Rev.* **2002**, *54*, 37–51.

(6) Choi, S.; Kim, S. W. Controlled Release of Insulin from Injectable Biodegradable Triblock Copolymer Depot in ZDF Rats. *Pharm. Res.* **2003**, *20*, 2008–2010.

10.1021/mp800087t CCC: $40.75
Published on Web 01/21/2009

In recent decades, a number of attempts have been made to overcome the limitations and drawbacks of conventional delivery of insulin by injection.[5−7] Long-term insulin delivery, ranging from weeks to months, can enhance patient compliance and convenience. For example, sustained subcutaneous insulin release systems can decrease the frequency of insulin injections, increase patient compliance, and reduce complications associated with poor glucose control.[8,9]

Microencapsulation technologies have advanced significantly during the past few decades, leading to many successful commercial products.[10−12] Maintaining the functional integrity of encapsulated insulin, however, is not easy due to the high sensitivity of insulin to the harsh conditions that can occur during the microencapsulation process.[13] For example, insulin-loaded microspheres have been produced by the double emulsion-solvent extraction/evaporation method.[14−16] Insulin microencapsulated in these microspheres frequently becomes unstable and can easily become denatured upon prolonged exposure to stressful conditions, such as a large water−organic solvent interface, high shear stresses, hydrophobic microenvironments, and elevated temperatures. Despite this instability, however, subcutaneous administration of insulin-loaded microspheres to diabetic mice reduced blood glucose levels, but most of the activity was lost within 100 h.[17,18]

Although advances have been made in preserving insulin stability and achieving extended release profiles, the complexity of emulsion-based encapsulation methods introduces problems that have yet to be solved. There is thus a need to develop new microencapsulation techniques that can reduce the exposure of encapsulated insulin to deleterious environments and that can encapsulate insulin under simple and mild conditions.

Several new strategies have been developed to improve insulin microencapsulation.[19−21] Recently, a coaxial ultrasonic atomizer was shown to generate reservoir-type microcapsules in a simple, mild, and highly efficient manner.[22,23] The prepared microcapsules have a spherical shape and small size, offering optimal surface-to-volume ratio and diffusion capacity. Because of its simplicity relative to ultrasonic methods, a monoaxial nozzle ultrasonic atomizer approach may provide significant advances in making microcapsules containing stable insulin. We have therefore used a monoaxial nozzle ultrasonic atomizer to prepare insulin-loaded microcapsules. We also tested whether these insulin-loaded microcapsules are active by subcutaneously administering them to insulin-dependent type 1 diabetic rats. We assessed the duration of insulin action and the host tissue response to determine whether insulin-loaded microcapsules could be used for sustained in vivo insulin delivery.

2. Results

Microencapsulation. A concentric nozzle ultrasonic atomizer was used to form microcapsules. When two different solutions were mixed, a water/oil (w/o) emulsion was formed within a few seconds. The atomization process

(7) Kashyap, N.; Viswanad, B.; Sharma, G.; Bhardwaj, V.; Ramarao, P.; Ravi Kumar, M. N. V. Design and evaluation of biodegradable, biosensitive in situ gelling system for pulsatile delivery of insulin. *Biomaterials* **2007**, *28*, 2051–2060.
(8) Colquitt, J. L.; Green, C.; Sidhu, M. K.; Hartwell, D.; Waugh, N. Clinical and cost-effectiveness of continuous subcutaneous insulin infusion for diabetes. *Health Technol. Assess.* **2004**, *8*, 1–171.
(9) Wu, J.; Wei, W.; Wang, L. Y.; Su, Z. G.; Ma, G. H. A thermosensitive hydrogel based on quaternized chitosan and poly(ethylene glycol) for nasal drug delivery system. *Biomaterials* **2007**, *28*, 2220–2232.
(10) Shi, Y.; Li, L. C. Current advances in sustained-release systems for parenteral drug delivery. *Expert Opin. Drug Delivery* **2005**, *2*, 1039–1058.
(11) de Vos, P.; Faas, M. M.; Strand, B.; Calafiore, R. Alginate-based microcapsules for immunoisolation of pancreatic islets. *Biomaterials* **2006**, *27*, 5603–5617.
(12) Freitas, S.; Merkle, H. P.; Gander, B. Microencapsulation by solvent extraction/evaporation: reviewing the state of the art of microsphere preparation process technology. *J. Controlled Release* **2005**, *102*, 313–332.
(13) Taluja, A.; Bae, Y. H. Role of a novel excipient poly(ethylene glycol)-*b*-poly(L-histidine) in retention of physical stability of insulin at aqueous/organic interface. *Mol. Pharmaceutics* **2007**, *4*, 561–570.
(14) Ibrahim, M. A.; Ismail, A.; Fetouh, M. I.; Göpferich, A. Stability of insulin during the erosion of poly(lactic acid) and poly(lactic-co-glycolic acid) microspheres. *J. Controlled Release* **2005**, *106*, 241–252.
(15) Kang, J.; Schwendeman, S. P. Pore Closing and Opening in Biodegradable Polymers and Their Effect on the Controlled Release of Proteins. *Mol. Pharmaceutics* **2007**, *4*, 104–118.
(16) Wang, X.; Wenk, E.; Hu, X.; Castro, G. R.; Meinel, L.; Wang, X.; Li, C.; Merkle, H.; Kaplan, D. L. Silk coatings on PLGA and alginate microspheres for protein deliver. *Biomaterials* **2007**, *28*, 4161–4169.
(17) Caliceti, P.; Veronese, F. M.; Lora, S. Polyphosphazene microspheres for insulin delivery. *Int. J. Pharm.* **2002**, *11*, 57–65.
(18) Furtado, S.; Abramson, D.; Simhkay, L.; Wobbekind, D.; Mathiowitz, E. Subcutaneous delivery of insulin loaded poly(fumaric-*co*-sebacic anhydride) microspheres to type 1 diabetic rats. *Eur. J. Pharm. Biopharm.* **2006**, *63*, 229–236.
(19) Luca, G.; Calvitti, M.; Nastruzzi, C.; Bilancetti, L.; Becchetti, E.; Angeletti, G.; Mancuso, F.; Calafiore, R. Encapsulation, in vitro characterization, and in vivo biocompatibility of Sertoli cells in alginate-based microcapsules. *Tissue Eng.* **2007**, *13*, 641–648.
(20) Dufrane, D.; van Steenberghe, M.; Goebbels, R. M.; Saliez, A.; Guiot, Y.; Gianello, P. The influence of implantation site on the biocompatibility and survival of alginate encapsulated pig islets in rats. *Biomaterials* **2006**, *27*, 3201–3208.
(21) Miura, S.; Teramura, Y.; Iwata, H. Encapsulation of islets with ultra-thin polyion complex membrane through poly(ethylene glycol)-phospholipids anchored to cell membrane. *Biomaterials* **2006**, *27*, 5828–5835.
(22) Yeo, Y.; Park, K. A new microencapsulation method using an ultrasonic atomizer based on interfacial solvent exchange. *J. Controlled Release* **2004**, *100*, 79–88.
(23) Park, J. H.; Ye, M.; Yeo, Y.; Lee, W.-K.; Paul, C.; Park, K. Reservoir-Type Microcapsules Prepared by the Solvent Exchange Method: Effect of Formulation Parameters on Microencapsulation of Lysozyme. *Mol. Pharmaceutics* **2006**, *3*, 135–143.

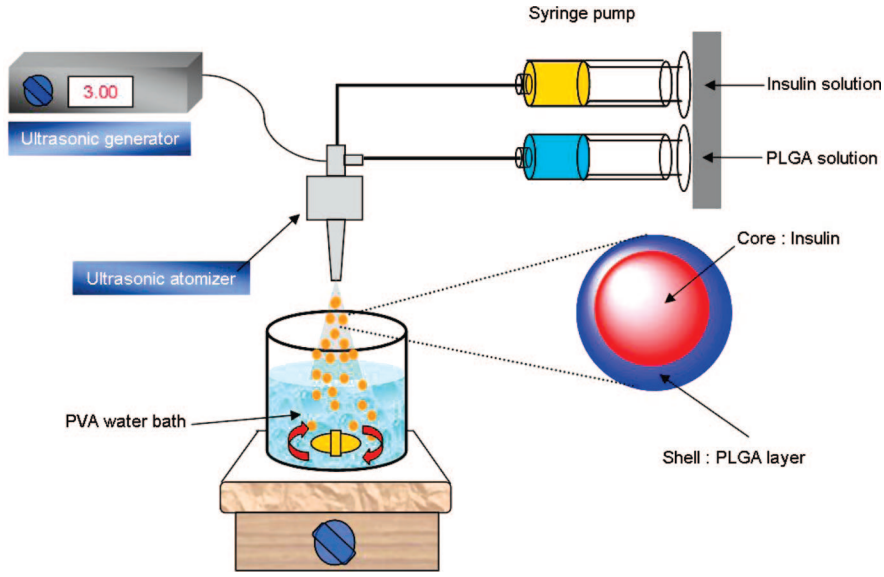

Figure 1. Schematic description of the microencapsulation method using a monoaxial ultrasonic atomizer.

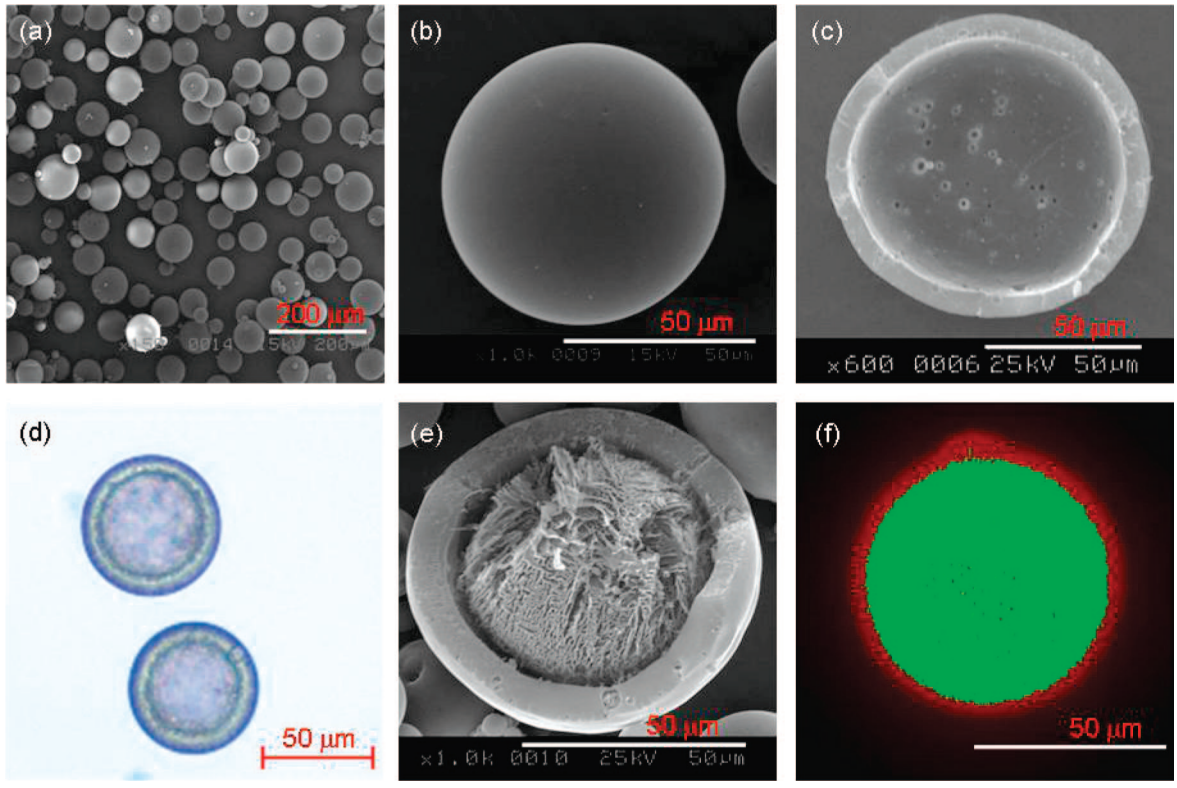

Figure 2. SEM pictures of (a) freeze-dried microcapsules, (b) one microcapsule, and (c) one cross-sectioned microcapsule. (d) Light microscopic image of insulin-loaded microcapsules, (e) SEM image of a cross-sectioned insulin-loaded microcapsule, and (f) confocal laser microscopic image of FITC-insulin-loaded microcapsules with nile red PLGA.

resulted in the formation of microdroplets of aqueous solution surrounded by poly(lactic-*co*-glycolic acid) (PLGA) solution (Figure 1). Scanning electron microscopy (SEM) analysis (Figure 2a and b) demonstrated that these procedures resulted in spherical microcapsules with a smooth surface structure. Particle size analysis showed that the mean particle size was 50 μm (range 30−90 μm). A cross-sectional image of these freeze-dried microcapsules clearly shows an inner core surrounded by a PLGA shell (Figure 2c); for insulin-loaded microcapsules, the insulin aqueous solution was surrounded by the PLGA shell (Figure 2d and e). The insulin encapsulation efficiency was 49%. A confocal laser microscopic image taken of microcapsules formed using fluorescein isothio-

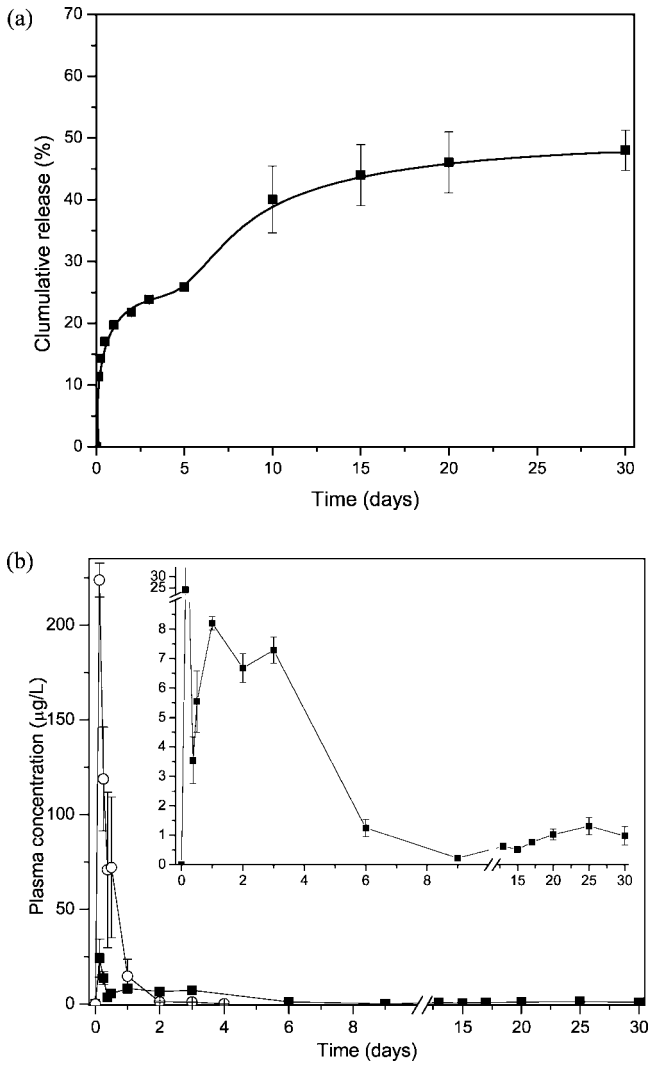

Figure 3. (a) Insulin release in vitro and (b) plasma insulin concentration in STZ-induced diabetic rats for 30 days after injection with (○) insulin solution or (■) insulin-loaded microcapsules.

cyanate (FITC)-insulin and nile red mixed with PLGA in ethyl acetate shows that the insulin cores were green while the PLGA shells were red (Figure 2f).

Insulin Release In Vitro. Measurement of the in vitro insulin release profile over 30 days showed that, after 24 h, approximately 20% of the insulin had been released from the microcapsules, indicative of an initial burst of insulin from the microcapsules (Figure 3a). Approximately 40% of the insulin had been released after 10 days and approximately 50% after 30 days, indicative of biphase release profiles. The remaining insulin (about 40% of the total) was detected after extraction of the microcapsules after 30 days.

Insulin Release In Vivo. The microcapsule solutions were easy to handle and easily penetrated by microsurgical needles. To measure insulin release from insulin-loaded microcapsules in vivo, we monitored plasma insulin concentrations in diabetic rats over time. We detected plasma insulin for up to 2 days in rats injected with insulin solution only (Figure 3b). The plasma insulin concentration in these rats reached a maximum after 3 h and then rapidly declined, reaching near zero levels after 2 days. In contrast, plasma insulin in rats injected with insulin-loaded microcapsules increased rapidly, reaching a maximum within 6 h, and was sustained for 30 days. The initial burst observed at 1 day was similar to the rapid burst observed during in vitro release, although insulin diffusion was likely faster in vivo than in vitro.

Table 1. Bioavailability of Insulin after Subcutaneous Injection of Insulin Solution Only and Insulin-Loaded Microcapsules

administration formulation	$AUC_{0\text{-}t}$ (μg/L)[a]	bioavailability (%)[b]
insulin-loaded microcapsules	R1-64.0	57.2[c]
	R2-46.2	41.3[c]
	R3-60.6	54.2[c]
	R4-56.2	50.2[c]
	avg 56.8 ± 3.9[d]	avg 50.7 ± 6.9[d]
insulin solution only	R1-120	100
	R2-116	
	R3-96	
	R4-117	
	avg 112 ± 11[d]	

[a] Evaluation time is 30 and 4 days for insulin-loaded microcapsules and insulin solution only, respectively. [b] Bioavailability = (AUC value for each insulin-loaded microcapsule administration)/(mean AUC value for direct insulin administration). [c] $P < 0.001$ versus insulin solution only. [d] Average represents the mean ± SD ($n = 4$).

$AUC_{0\text{-}t}$ values, calculated by measuring the area under the plasma insulin curves (AUC) using the trapezoidal rule, and absolute bioavailability of insulin were measured from the plasma concentration profiles (Table 1). Using insulin-loaded microcapsules, the $AUC_{0\text{-}t}$ was 57 ± 4 μg/L. The absolute bioavailability of insulin-loaded microcapsules compared with insulin solution was about 51%.

Blood Glucose Levels. When we measured the average blood glucose levels over time for rats administered insulin solution and insulin-loaded microcapsules, we found that, after 3 h, both the solution and the microcapsules reduced glycemia to normal blood glucose levels (Figure 4). Rats injected with insulin solution maintained blood glucose levels within the normal range for about 1 day, after which glycemia slowly increased, with starting hyperglycemic values achieved within 3 days. In contrast, the insulin-loaded microcapsules reduced blood glucose levels to 80 mg/dL at 3 h after administration. Over the following 3 days, blood glucose concentrations increased to 200 mg/dL and were then maintained at about 100−200 mg/dL for 55 days.

Conformational and Bioactivity Stability of Insulin. To assess the structural integrity of encapsulated insulin, we applied circular dichroism (CD) spectroscopy. We found that the CD spectrum of insulin encapsulated inside insulin-loaded

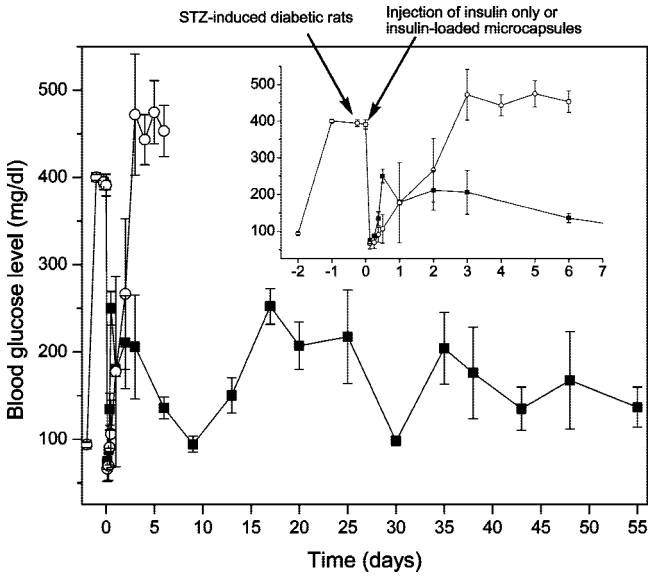

Figure 4. Blood glucose levels in STZ-induced diabetic rats after injection with (○) insulin solution or (■) insulin-loaded microcapsules.

microcapsules was virtually indistinguishable from that of a native insulin solution.[24]

To examine the in vivo biologic action of insulin released from insulin-loaded microcapsules for the experimental period, the insulin-loaded microcapsules were injected into STZ-induced diabetic rats. The microcapsules were removed from rats at 3, 7, and 25 days. We then measured the average blood glucose levels for rats before and after removing the microcapsules. Under the administration of insulin-loaded microcapsules, blood glucose levels maintained at about 100−200 mg/dL. However, blood glucose concentrations increased to 300−400 mg/dL after removal of insulin-loaded microcapsules.[25]

In Vivo Fluorescence Imaging. Fluorescent images were acquired from a nude mouse after subcutaneous injection of FITC-insulin-loaded microcapsules (Figure 5). High levels of green fluorescence were observed at the injection site, with diffusion after injection (Figure 5a). The area of fluorescence increased from 30 to 120 min (Figure 5b−d), with a maximal area observed at 3 h after administration, probably due to the in vivo burst effect. At 2 days, the image area decreased and reached the area of initially injected microcapsules. After this time, both the intensity and area of fluorescence gradually decreased. Negligible fluorescence intensity was observed after 21 days, and none after 28 days. FITC-insulin-loaded microcapsules removed from a rat after 28 days showed a homogeneous distribution of fluorescence (Figure 6), with about 30% of the FITC-insulin retained by the microcapsules after 28 days.

(24) CD spectra of native insulin and encapsulated are illustrated in the Supporting Information (Figure S1).

(25) Blood glucose levels before and after removal of insulin-loaded microcapsules are illustrated in the Supporting Information (Figure S2).

SEM Morphology of the In Vivo Microcapsules. Insulin-loaded microcapsules removed from rats after 1 and 28 days were frozen in liquid nitrogen, freeze-dried, and observed by SEM (Figure 7). One day after implantation, the microcapsules were spherical. After 28 days, the microcapsules were interspersed with connective tissue. They remained round in shape, although they showed a slightly crushed spherical structure.

Host Tissue Response. The microcapsules could be easily identified and isolated from the surrounding tissue. Microcapsule optical DIC showed that, as time after transplantation increased, the area of the microcapsules decreased and the tissue became more organized (Figure 8). The tissues supported the interface area of the microcapsules, which were well integrated with the surrounding tissue. At 4 weeks, the microcapsules were uniformly covered with tissue, and adherence to the surrounding tissue was more evident. Fragments of the microcapsules were interspersed with connective tissue, and there were numerous fibrous tissues beneath the interface area of the microcapsules.

To assess their local biocompatibility with the PLGA microcapsules, tissues into which the microcapsules had been transplanted were examined. Response to the macrophage marker ED1 antibody is considered a unique in vivo indicator of inflammatory response.[21] Tissue was therefore stained with ED1 and DAPI to characterize the extent of host cell infiltration and inflammatory cell accumulation within and near the transplanted microcapsules (Figure 8). DAPI staining (blue) showed many host cells surrounding the PLGA microcapsules, and ED1 staining (red) showed macrophage accumulation at the surfaces of the PLGA microcapsules and in surrounding tissues after 1 week. Macrophages may act to remove the microcapsules from the injection site. The tissue adjacent to the microcapsules showed a significant increase in ED1 positive cells at 2 weeks, but the number decreased after 3 weeks, with a marked decrease in macrophages after 4 weeks.

Hematoxylin and eosin (H&E)-stained histological sections of harvested microcapsules showed that, after 1 week, the numbers of macrophages and neutrophils had increased in the border zone and near the microcapsules as well as inside the tissue layer (Figure 9). The microcapsules had been invaded by host cells, and there was a dense accumulation of inflammatory cells, including some giant cells, around each microcapsule. In agreement with the ED1 assay results, cell infiltration peaked at 2 weeks and thereafter decreased over time, indicating that the transplantation of foreign materials resulted in an acute short-term inflammatory response. As time after transplantation increased, there was little evidence of focal foreign body reactions, with few neutrophils, coupled with formation of normal fibroblasts below the tissue layer.

3. Discussion

In insulin-dependent type 1 diabetic patients, daily injection of external insulin is required in order to achieve

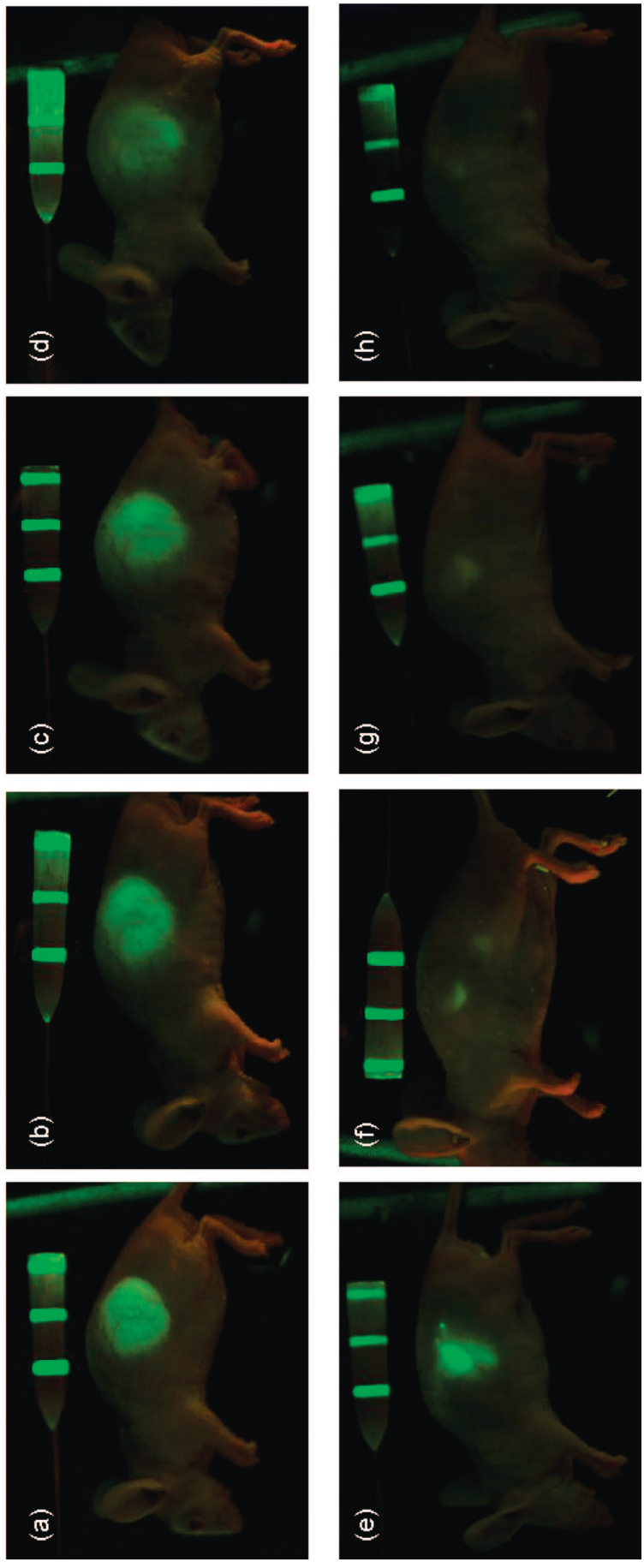

Figure 5. In vivo fluorescence image of a nude mouse injected with FITC-insulin-loaded microcapsules taken (a) 2 min, (b) 30 min, (c) 60 min, (d) 120 min, (e) 2 days, (f) 1 week, (g) 2 weeks, and (h) 3 weeks after initial injection. (Line represents 1 cm.)

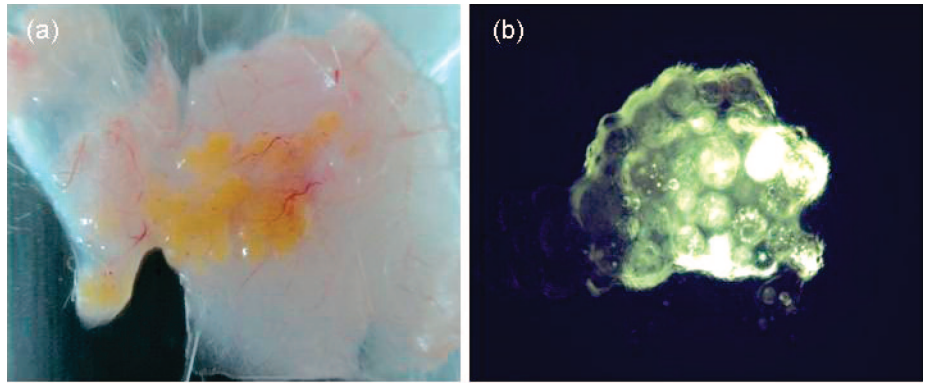

Figure 6. (a) Optical image and (b) fluorescence image of insulin-loaded microcapsules after 28 days.

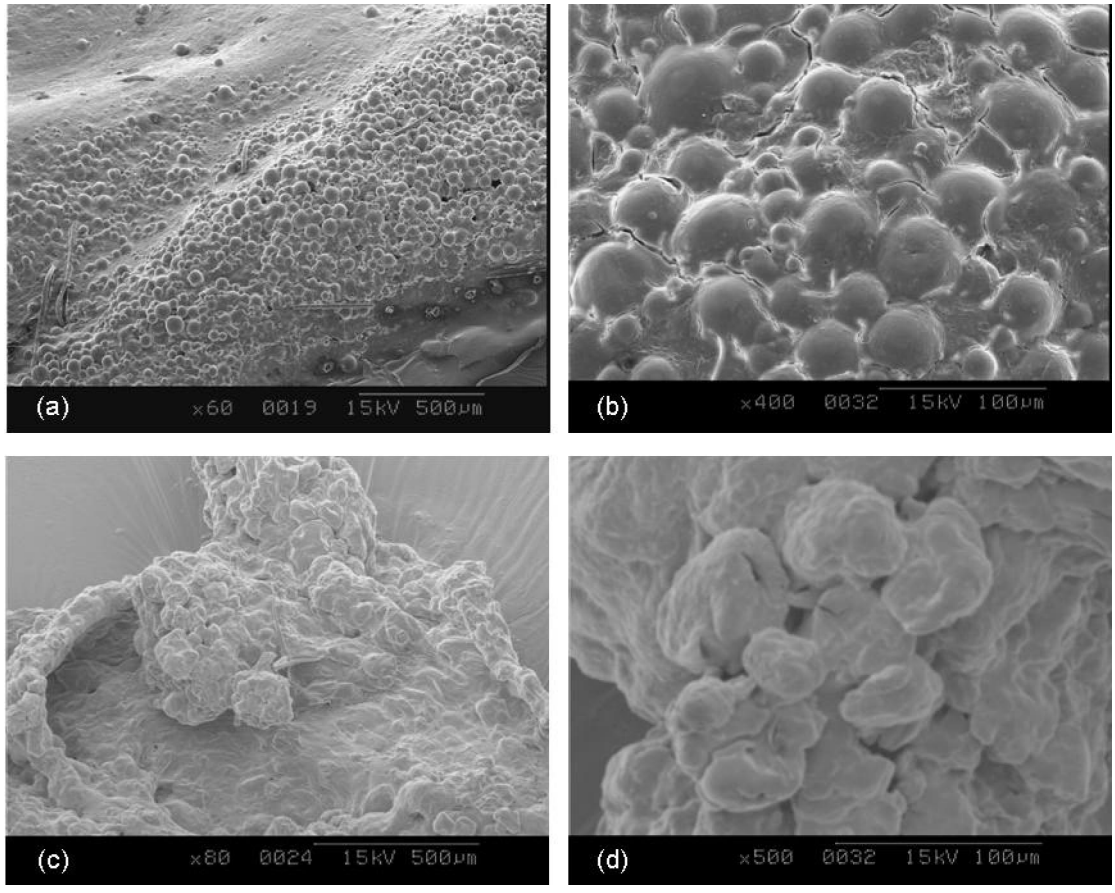

Figure 7. SEM images of insulin-loaded microcapsules after (a, b) 1 day and (c, d) 28 days.

normoglycemia. Because of difficulties in achieving physiological control of blood glucose concentrations, however, chronic and degenerative complications often occur. Thus, a successful alternative method for delivering therapeutic doses of insulin would improve the quality of life of many people who must routinely self-inject insulin. Because parenteral insulin has such a short half-life in blood (~4.5 min),[26] frequent insulin injections are required. Various approaches have been tried to extend the in vivo fate of insulin.[23,27−29] Insulin-loaded microcapsule transplantation has recently emerged as an attractive alternative to daily insulin injections for patients with type 1 diabetes, and as a promising clinical modality.[30,31]

(26) Attia, N.; Jones, T. W.; Holcombe, J.; Tamborlane, W. V. Comparison of human regular and lispro insulins after interruption of continuous subcutaneous insulin infusion and in the treatment of acutely decompensated IDDM. *Diabetes Care* **1998**, *21*, 817–821.

(27) Kwon, Y. M.; Kim, S. W. Biodegradable Triblock Copolymer Microspheres Based On Thermosensitive Sol−Gel Transition. *Pharm. Res.* **2004**, *21*, 339–343.

(28) Takenaga, M.; Yamaguchi, Y.; Kitagawa, A.; Ogawa, Y.; Kawai, S.; Mizushima, Y.; Igarashi, R. Optimum formulation for sustained-release insulin. *Int. J. Pharm.* **2004**, *271*, 85–94.

(29) Taluja, A.; Bae, Y. H. Role of a novel excipient poly(ethylene glycol)-*b*-poly(L-histidine) in retention of physical stability of insulin in aqueous solutions. *Pharm. Res.* **2007**, *24*, 1517–1526.

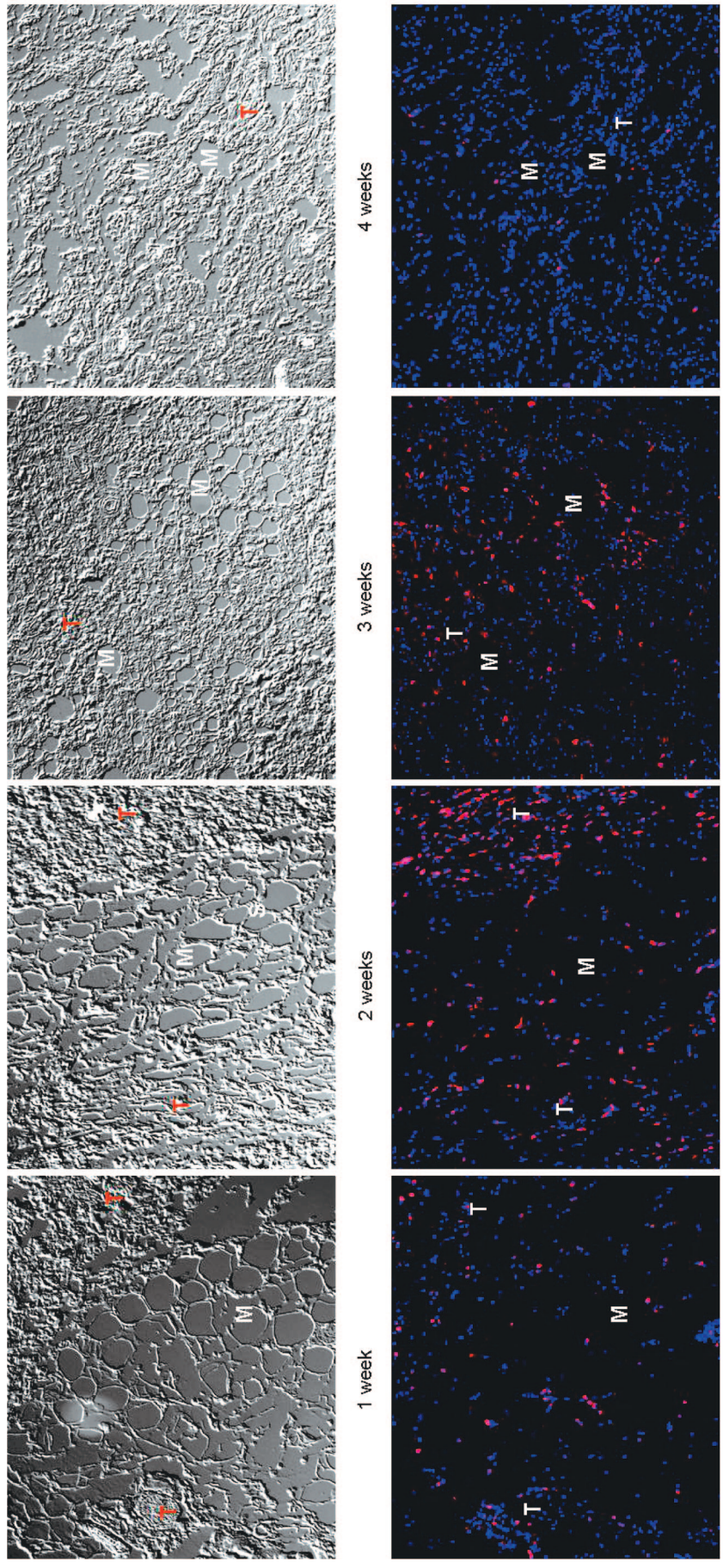

Figure 8. ED1 immunofluorescent staining of insulin-loaded microcapsules. T and M indicate tissue and microcapsules, respectively. (Upper) DIC images; (lower) immunohistochemical images.

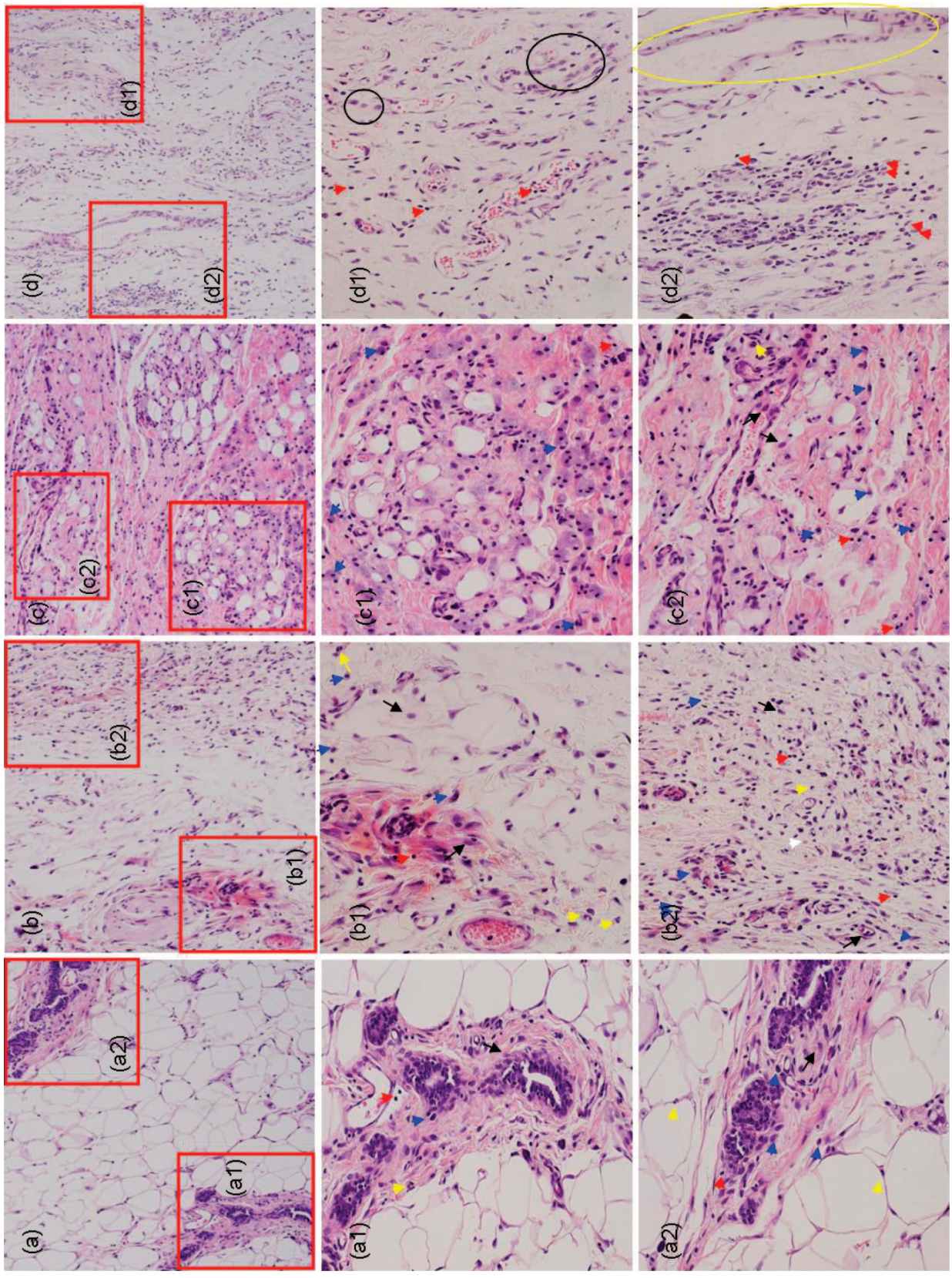

Figure 9. H&E staining of insulin-loaded microcapsules (a) 1 week, (b) 2 weeks, (c) 3 weeks, and (d) 4 weeks after injection. Magnification for the first row is ×40 and for the second and third rows is ×100. The yellow, red, blue, and black arrows represent neutrophils, lymphocytes, macrophages, and foreign body giant cells, respectively. Circles indicate normal fibroblasts.

It was found that a coaxial ultrasonic atomizer produced microcapsules in a simple and highly efficient manner.[22,23] The use of a monoaxial nozzle ultrasonic atomizer to form microcapsules in this work has not been previously reported. Using this monoaxial ultrasonic atomizer and a mixture of PLGA and insulin solutions, insulin-loaded microcapsules could be formed within a few seconds. These microcapsules, about 50 μm in diameter, have an insulin core inside a PLGA shell.

Maintenance of the structural integrity of insulin during encapsulation in microcapsules is crucial for its biological efficacy. This method can provide its limited exposure to a water−organic solvent interface area and the lack of stressful conditions. The secondary structure of insulin within microcapsules and native insulin was investigated using CD. The CD spectrum of the encapsulated insulin is almost the same as that of native insulin, suggesting that the structure of encapsulated insulin in microcapsules is preserved during the encapsulation process. Thus, the insulin microencapsulated by this method can remain stable.

We found that insulin was released in vitro from these microcapsules by two-phase kinetics: a fast initial burst on the first day, followed by a slow, smooth release for up to 30 days. In vivo, in diabetic rats, an initial insulin burst was also observed, similar to the in vitro burst. During this initial burst release, it is likely that the insulin in the PLGA layer molecularly dispersed throughout the microcapsules was rapidly perfused by the releasing buffer under biologic conditions. Most of the insulin, however, is present inside the microcapsules and is therefore not easily available to the releasing buffer. Insulin inside the microcapsules is released at a very slow rate for up to 30 days, both in vitro and in vivo, indicating that microencapsulating insulin can increase the duration of insulin release.

In contrast to the microcapsules, injection of insulin solution results in a rapid increase in plasma insulin concentration, which substantially disappears after 3 days. Both insulin solution and microcapsules, however, show similar initial behavior in lowering plasma glucose levels, indicating that the microencapsulated insulin retains its biological activity. The rapid decrease in plasma glucose levels obtained with insulin-loaded microcapsules is likely due to the initial insulin burst. However, release of the remaining insulin, which is entrapped in the aggregate state in the microcapsules, takes place more slowly, with lower plasma glucose levels maintained for at least 55 days. The target values for plasma glucose levels recommended by the American Diabetes Association are 80−120 mg/dL for fasting preprandial conditions and 100−140 mg/dL at bedtime. Insulin-loaded microcapsules maintained blood glucose concentrations at about 100−200 mg/dL. Because the diabetic rats in this study were fed continuously, the levels of blood insulin and glucose do not directly coincide; however, these results indicate that insulin-loaded microcapsules can be effectively used for extended periods to treat this experimental model of type 1 diabetes.

During administration of insulin-loaded microcapsules, the blood glucose level in diabetic rats was almost constant (about 100−200 mg/dL). However, blood glucose levels after removal of insulin-loaded microcapsules again increased to hyperglycemic levels and then maintained at 300−450 mg/dL. In the case of the removal of microcapsules at day 25, the rat died of hyperglycemic shock after 2 days. Therefore, this result directly indicates that the insulin released from the insulin-loaded microcapsules can control blood glucose levels in type 1 diabetic rats and maintain its biological activity without any significant change after loading and in vivo release.

Molecular imaging is a relatively new method to assess in vivo processes without excising tissue from living animals.[32,33] In recent years, there have been major advances in available reporter probes and the corresponding devices used to detect them. We therefore used this method to assess in vivo insulin release. Our results provide further evidence that molecular imaging of FITC-labeled insulin will likely be increasingly important for monitoring insulin noninvasively.

Although PLGA has been widely used in clinical medicine as FDA approved material, these polymers eventually degrade directly to acid, leading to undesirable inflammatory responses[34,35] and susceptibility of PLGA microcapsules to inflammatory damage. To our knowledge, however, little previous effort has been devoted to examining host tissue responses to implants as we have done using immunohistochemical staining with ED1 as an anti-CD68 antibody to identify infiltrating macrophages following implantation of PLGA microcapsules in vivo. Staining with the macrophage marker ED1 and H&E revealed that the tissues surrounding the PLGA microcapsules contained macrophages and neutrophils. This acute inflammatory response to PLGA was associated with a destructive neutrophil action. Over time, however, there was a marked decrease in macrophages and neutrophils. In addition, these microcapsules showed infiltration by and ingrowth of host cells, along with adequate engraftment within the host tissue. Our findings, showing

(30) Zhong, Y.; Bellamkonda, R. V. Dexamethasone-coated neural probes elicit attenuated inflammatory response and neuronal loss compared to uncoated neural probes. *Brain Res.* **2007**, *1148*, 15–27.

(31) Takenaga, M.; Yamaguchi, Y.; Ogawa, Y.; Kitagawa, A.; Kawai, S.; Mizushima, Y. Administration of optimum sustained-insulin release PLGA microcapsules to spontaneous diabetes-prone BB/Wor//Tky rats. *Drug Delivery* **2006**, *13*, 149–157.

(32) Matthäus, C.; Kale, A.; Chernenko, T.; Torchilin, V.; Diem, M. New Ways of Imaging Uptake and Intracellular Fate of Liposomal Drug Carrier Systems inside Individual Cells, Based on Raman Microscopy. *Mol. Pharmaceutics* **2008**, *5*, 287–293.

(33) Kim, J. H.; Park, K.; Nam, H. Y.; Lee, S.; Kim, K.; Kwon, I. C. Polymers for bioimaging. *Prog. Polym. Sci.* **2007**, *32*, 1031–1053.

(34) Zhao, X.; Jain, S.; Benjamin, L. H.; Gonzalez, S.; Irvine, D. J. Directed cell migration via chemoattractants released from degradable microspheres. *Biomaterials* **2005**, *26*, 5048–5063.

(35) Jilek, S.; Walter, E.; Merkle, H. P.; Corthesy, B. Modulation of allergic responses in mice by using biodegradable poly(lactide-*co*-glycolide) microspheres. *J. Allergy Clin. Immunol.* **2004**, *114*, 943–950.

minimal inflammation after implantation of insulin-loaded microcapsules, suggest that these microcapsules may be safe and biocompatible in vivo and may be candidates for clinical development.

4. Conclusion

We prepared insulin-loaded microcapsules, consisting of an insulin core inside a PLGA shell, using a monoaxial ultrasonic atomizer. A solution containing these microcapsules could be easily injected by a microsurgical needle into type I diabetic rats. Sustained insulin release from these insulin-loaded microcapsules was observed, as well as long-term pharmacological duration of insulin activity, as shown by reduction of glycemia to normoglycemia. Moreover, the inflammatory response observed initially was reduced over time. Although future studies will be needed to eliminate the hypoglycemic risk associated with an insulin burst, we believe this method of microcapsule formation provides a useful experimental platform for sustained in vivo pharmacological performance of protein drugs.

5. Experimental Section

Materials. Low molecular weight PLGA (lactic/glycolic acid = 50/50, MW = 14 500) was purchased from Birmingham Polymers, Inc. (Birmingham, AL). Poly(vinyl alcohol) (PVA, 87−89% hydrolyzed, MW = 85 000−124 000) purchased from Sigma (Milwaukee, WI) was used as an emulsifier. Bovine insulin (Zn salt, 28.8 IU/mg) was purchased from Sigma. Fluorescein isothiocyanate (FITC)-labeled insulin and nile red were purchased from Sigma (St. Louis, MO). All other chemicals were analytical grade and used without further purification.

Microencapsulation of Insulin Using Monoaxial Ultrasonic Atomizer. Microcapsules were generated by using a monoaxial ultrasonic atomizer (Sono-Tek Corp, Milton, NY). PLGA solution in ethyl acetate and an aqueous solution containing insulin were separately fed into an ultrasonic atomizer with a monoaxial nozzle at defined flow rates. In all experiments, the flow rates of the PLGA solution and the insulin aqueous solution were fixed to 4 and 0.2 mL/min, respectively. PLGA and insulin were dissolved in ethyl acetate and 0.1 N hydrochloric acid, respectively. The concentrations of PLGA and insulin solution were 3 and 5 w/v %, respectively. Microdroplets were produced by atomizing the mixed solutions of PLGA and insulin within a few seconds at a vibration frequency of 60 kHz, and they were then collected in a 1 w/v % PVA solution for 2 min. The distance between the atomizer head and the aqueous PVA solution was 1 cm, and the stirring speed of the PVA solution was 1000 rpm. The resulting solutions were left with gentle stirring for 2 h to allow solidification of the microcapsules, followed by washing with distilled water. The solution was frozen at −74 °C, followed by freeze-drying for 4−7 days. The morphology of the obtained microcapsules was observed by using a CAMSCOPE (Sometech, Korea) and an optical microscope (Nikon, Labophot-2, Japan). The particle sizes of microcapsules were measured by using a particle size analyzer (BI-DCP Particle Sizer, U.K.).

Confocal Laser Scanning Microscopy (CLSM). For the sample preparation, FITC-insulin-loaded microcapsules were produced using 5 w/v % FITC-insulin in aqueous solution and 0.003% nile red in the 3 w/v % PLGA solution in ethyl acetate. Before the measurements, they were thoroughly washed with distilled water. The structure of the microcapsule was examined using a laser scanning confocal imaging system (model LSM-510 Pascal, Carl Zeiss, Germany) equipped with an argon/HeNe laser and a Zeiss LSM 510 inverted microscope. All confocal fluorescence pictures for FITC-insulin and nile red were taken with a ×20 objective lens and excitation at 488 and 568 nm, respectively.

Encapsulation Efficiency of Insulin-Loaded Microcapsules. The encapsulation efficiency of insulin was determined using CH_2Cl_2 and distilled water. Microcapsules (10 mg) were placed into a test tube to which CH_2Cl_2 (0.2 mL) was added to dissolve the polymer portion of the microcapsules. Then, 0.8 mL of distilled water was added to allow solubilization of the insulin. The resulting mixture was sonicated for 90 min at 25 °C and centrifuged at 10 000 rpm for 5 min. The amount of insulin was analyzed using a reverse-phase high-performance liquid chromatography (RP-HPLC) system equipped with a model P-2000 pump, a model AS-3000 auto sampler, and a model UV-1000 UV detector at 280 nm (Thermo Separation Products, Fremont, CA). The column used was Shodex RSpak (200 × 4 mm, RP18-415, 5 μm). The mobile phase was composed of a distilled water, acetonitrile, and tetrafluoroacetic acid (70:30:0.1 v/v) mixture, and the flow rate of that was adjusted at 1.0 mL/min. The encapsulation efficiency (E) was defined as follows:

$$E = [(\text{amount of encapsulated insulin})/(\text{total amount of feed insulin})] \times 100$$

Conformational Stability of Insulin. The insulin solution (pH 7.4, phosphate buffer solution (PBS)) as mentioned in the above section was collected. As a control, native insulin solution was prepared. The conformational characteristics of insulin were measured on a Jasco-715 CD spectrophotometer (Tokyo, Japan).

Insulin Release In Vitro. Microcapsule-containing vials (0.1 g microcapsules, $n = 5$) were suspended in 5 mL of PBS (pH 7.4) and shaken at 100 rpm and 37 °C. At predetermined time intervals, 500 μL of the supernatant was collected in the microcapsule suspension. Fresh PBS (500 μL) was then added to the microcapsule suspension. The amount of released insulin was determined by RP-HPLC as described in the previous section. The amount of cumulatively in vitro released insulin was calculated by comparison with the standard calibration curves prepared with known concentrations of insulin.

Animal Models. Sixteen Sprague−Dawley (SD) rats (320−350 g, 8 weeks) were used in the release tests. The rats were housed in sterilized cages with sterile food and water and filtered air, and were handled in a laminar flow hood following aseptic techniques. All animals were treated

in accordance with the Catholic University of Korea Council on Animal Care Guidelines. Blood glucose levels were monitored using a commercial glucose meter (AccuCheck Advantage). Results are presented in units of mg/dL (range 10−600 mg/dL). Glucose levels on day 0 prior to treatment ranged from 98−105 mg/dL. On day 0, streptozotocin (STZ) (40 mg/kg) in citrate buffer (pH 4.5) was given by intraperitonial injection to male SD rats to induce hyperglycemia. The glucose levels were measured on day 1 and day 2 before experiment, and rats which had glucose levels of 380−420 mg/dL were used for experiment. Nine SD rats (320−350 g, 8 weeks) were used as STZ-induced diabetic rats as a control model to verify diabetes. Five STZ-induced diabetic rats that did not receive an injection died within 3 weeks of hyperglycemia, and four rats survived for 4 weeks; blood glucose concentrations of these longest-surviving rats were maintained at about 350−500 mg/dL.[36] Additionally, to examine the biologic action and bioactivity of insulin released from insulin-loaded microcapsules, three STZ-induced diabetic rats received an injection of insulin-loaded microcapsules. The microcapsules were removed from the rats after 3, 7, and 25 days. Their blood glucose levels were monitored using an AccuCheck Advantage meter for 30 days.

Insulin Release In Vivo. Just before administration, the formulation of insulin-loaded microcapsules was dispersed (20%, w/v) with 5% D-mannitol containing 2% carboxymethylcellulose and 0.1% Tween 80 as an IU vehicle. On day 2 after rats received STZ, 1 mL (190 IU/kg body weight of rat) of the microcapsule solution was injected using a 1 cc syringe with a 26-gauge needle into the subcutaneous dorsum of diabetic rats that had been anesthetized with ethyl ether.

Four rats were used for each group of normal rat, dietetic rats without any injection, and dietetic rats with insulin only and insulin-loaded microcapsules. For the in vivo detection of plasma insulin, an aliquot of blood was drawn from the tail vein of each rat at specified blood collection times. These samples were all taken in the morning (9:00−11:30 a.m.), except for that taken up to 48 h after injection, until the 55th day. A 0.3 mL aliquot of blood from the catheterized tail vein was collected in an Eppendorf tube and mixed with 0.2 mL of a 1:499 mixture of heparin and saline, followed by vortexing. To obtain plasma, the blood solution was centrifuged at 10 000 rpm for 5 min at room temperature. To the plasma obtained in this way, distilled water (100 μL), 66 mM EDTA (300 μL), and 50 mM HEPES (pH 7.4) (400 μL) were added. Plasma samples were stored frozen at −20°C until assayed. Plasma insulin concentration was determined using enzyme immunoassay kit (bovine insulin ELISA, Mercodia AB, Sweden). To run each assay, all reagents and samples were brought to room temperature. An aliquot from each sample (25 μL) was transferred to a well plate strip. After following the manufacturer's protocol, absorbance at 450 nm was measured with a microplate reader (EL808 ultra microplate reader; Bio-Tek Instrument). The amount of in vivo released insulin was calculated by comparison with the standard calibration curves prepared with known concentrations of insulin using the insulin ELISA kit. The area under the plasma insulin concentration versus time curve was calculated as AUC. the evaluation time for AUC is 30 and 4 days for insulin-loaded microcapsules and insulin solution only, respectively. The relative bioavailability was calculated by comparing the AUC of the insulin-loaded microcapsules to that of insulin solution only. To analyze the state of the plasma insulin and to examine the reliability of the method, we also recorded spectra in only blood obtained from normal or STZ-induced diabetic rats without any injection. There were significant differences between the blood of plasma insulin released from insulin-loaded microcapsules and the blood obtained from normal or STZ-induced diabetic rats without any injection.[37]

In Vivo Fluorescence Image. The microcapsules with FITC-labeled insulin were suspended in an injection vehicle. A male nude mouse at 5 weeks old was anesthetized with ethyl ether and treated with 15 mg of microcapsules via subcutaneous injections to the left dorsum using a 22-gauge needle. The image of the mouse was taken from the side view at the selected time, using a fluorescence imaging system (LT-9500 Illumatool Bright Light system, CA). Fluorescence images were taken in a wavelength range of 515 nm at an excitation wavelength of 470 nm. After digitization using a CCD, fluorescence images were visualized with Meta Image Series software (MetaMorph, Molecular Devices Corporation).

SEM Measurement of In Vitro and In Vivo Microcapsules. Scanning electron microscopy (SEM, S-2250N, Hitachi, Japan) was used to examine the morphology of the in vitro and in vivo microcapsules. The microcapsules removed from the rat were immediately mounted on a metal stub precooled in liquid nitrogen. After mounting of the microcapsules, the metal stub was quickly immersed in a liquid nitrogen bath to minimize alteration of the microcapsules. The stub then was freeze-dried at −75 °C using a freeze-dryer. Once completely dry, the sample on the metal stub was coated with a thin layer of platinum using a plasma-sputtering apparatus (Emitech, K575, Japan) under an argon atmosphere.

Histological Analysis. At 1, 2, 3, and 4 weeks after transplantation, the rats were sacrificed and the microcapsules were dissected individually and removed from the subcutaneous dorsum. The microcapsules were prepared for immunohistochemical analysis. The microcapsules were left in place, and the tissues were immediately fixed with 10% formalin and embedded in paraffin wax. Each embedded specimen was then sectioned (4 μm) along the longitudinal axis of the implant, and the sections were stained with DAPI (6-diamino-2-phenylindoadihydrochloride, Sigma), ED1 (mouse anti-rat CD68, Serotec, U.K.), and hematoxylin and

(36) Blood glucose levels in normal rats and in STZ-induced diabetic rats without any injection are illustrated in the Supporting Information (Figure S3).

(37) Plasma insulin concentrations are illustrated in the Supporting Information (Figure S3).

eosin (H&E). The staining procedures for DAPI and ED1 were as follows. The slides were washed with PBS-T (0.05% Tween 20 in PBS). The slides were blocked with buffer of 5% BSA (bovine serum albumin, Roche, Germany) and 5% HS (horse serum, GIBCO, Invitrogen) in PBS for 1 h at 37 °C. Sections were incubated with mouse anti-rat CD68 overnight at 4 °C. After washing with PBS-T, the slides were incubated with the secondary antibody (rat anti-mouse Alexa Fluor594, Invitrogen) for 3 h at room temperature in the dark. After washing with PBS-T, the slides were counterstained with DAPI and then mounted with a fluorescent mounting solution (DAKO, Denmark). Immunofluorescence images were visualized under an OLYMPUS IX81 microscope (Olympus, Japan) equipped with Meta Image Series software.

Data Analysis. The areas under individual plasma insulin concentration−time curves for a released time period (AUC_{0-t}) were calculated. Bioavailabilities were determined by dividing the AUC value for each insulin-loaded microcapsule administration by the mean AUC value for direct insulin administration into the subcutaneous dorsum of rats. Statistical analysis was performed using Student's *t* test.

Acknowledgment. This study was supported by a grant from KMOHW (A050082) and the Korea Science and Engineering Foundation (KOSEF) pioneer grant (M10711060001-08M1106-00110).

Supporting Information Available: Far-UV CD spectra of native and encapsulated insulin, blood glucose levels in STZ-induced diabetic rats before and after removal of insulin-loaded microcapsules, blood glucose levels in normal and STZ-induced diabetic rats without injection, and plasma insulin concentration in STZ-induced diabetic rats for 30 days after injection with insulin solution or insulin-loaded microcapsules. This material is available free of charge via the Internet at http://pubs.acs.org.

MP800087T